29th International Congress on Sound and Vibration
The annual congress of the International Institute of Acoustics and Vibration (IIAV)
9–13 July 2023
ICSV29

TONAL NOISE EMISSION BY A LOW-MACH LOW-REYNOLDS NUMBER PROPELLER INGESTING A BOUNDARY LAYER

Sébastien Guérin
Deutsches Zentrum für Luft- und Raumfahrt (DLR), Institute of Propulsion Technology, Berlin, Germany
e-mail: Sebastien.Guerin@dlr.de
Tobias Lade
Deutsches Zentrum für Luft- und Raumfahrt (DLR), Institute of Propulsion Technology, Berlin, Germany
email: Tobias.Lade@dlr.de
Leandro Castelucci
University of Twente, Drienerlolaan 5, 7522 NB, Netherlands
email: l.a.castelucci@utwente.nl
Ismaeel Zaman
Department of Aerospace Engineering, University of Bristol, Bristol, BS8 1TR, UK
email: iz16368@bristol.ac.uk

The emission of acoustic tones by a low Mach number and low Reynolds number 2-bladed propeller immersed up to 44% in a boundary layer developping over a flat plate is investigated for one operating condition near the peak efficiency. Microphone measurements in two different open-jet wind tunnels are compared to predictions, which are based on the acoustic analogy. The blade element momentum theory is applied to calculate the mean flow and the blade lift. The laminar–turbulent transition is considered in the process. The steady and unsteady loading mechanisms due to blade loading and rotor interaction with the boundary-layer velocity deficit, respectively, are modelled separately and superimposed linearly. The acoustic reflections by the plate are modelled with the method of image. The prediction results are in satisfactory agreement with the measurements, in particular, they confirm the growing contribution of BLI tones as the harmonic index of the blade passing frequency increases.
Keywords: propeller noise, boundary layer ingestion, BEMT

1. Introduction

Distributed electric propulsion (DEP) is presented as a solution to reduce the impact of air transport on global warming. It is most likely to be used for regional flights. DEP offers new possibilities in terms of airplane architecture and integration of the propulsion system. The impact of DEP on community noise is a thorny issue because of the interaction between the propulsion units and with the airframe. The European project ENODISE [1] aims at investigating some of the emerging acoustic topics through low TRL experiments and simulations. One of the generic configurations investigated in ENODISE is the subject of this study: it corresponds to a two-bladed propeller partially immersed in a boundary layer.

From experience, we know that a rotor becomes noisier when ingesting a boundary layer; above all, because of the interaction with the excess turbulence in the boundary layer. The deficit in mean velocity can also lead to increased broadband self-noise because of flow separation on the blade surface. It also induces a periodic blade loading, which is expected to act as an additional source of tonal noise.

The presence of humps in the spectral signature was also reported by Alexander, Devenport, Glegg et al. [3] for experiments performed at Virginia Tech on a low speed open rotor ingesting a boundary layer. The humps were centered at the blade passing frequency and its multiples. That effect is similar to that of turbulent eddies accelerated in the inlet of a fan. Hanson studied that mechanism and concluded [2]: "*Since these eddies are often many rotor diameters long, each one is chopped several times as it passes through the rotor. This causes partially coherent blade loading which leads to partially coherent or narrow-band random noise.*" Blade-to-blade coherence must be considered for reproducing that effect.

Later results from the Virginia Tech rig presented by Murray et al. [4] suggested the presence of an additional mechanism, which may have explained that the humps had become much more pronounced at high thrust. Based on some investigations in the tip clearance region, they concluded that sharp humps may have been due to the blade–vortex interaction (BVI) mechanism resulting from the boundary layer separation, which had produced large vortex structures.

Experiments at DLR on the low-speed fan test rig CRAFT were carried out for different inflow distortions created by means of perforated grids using different patterns. The results, published by Klähn et al. [5], indicate that fan noise is very sensitive to the choice of the distortion device. A cyclostationary analysis of the pressure signals was performed in order to remove the rotor-locked contribution. The results showed a significant effect of BLI on broadband noise. Regarding tonal noise, an increase of up to 7 dB was found [6]. This configuration is different from ENODISE and Virginia Tech in that the fan is ducted and the rotor–stator interaction is the dominant source of noise.

The present study is focused on tonal noise. Interestingly, the Virginia Tech experiments do not show any sharp tones, probably because the tonal emission is covered by broadband noise. On the contrary, the ENODISE experiments exhibit sharp tones but no strong humps around the blade passing frequency (BPF) tones [7, 8, 9]. The very low solidity may explain the difference between the two experiments.

Table 1: Comparison of key experimental parameters.

Benchmark case	D (mm)	B	tip clearance (% D)	max thickness (% chord)	solidity at 75% radius	U_∞ (m/s)	J
Virginia Tech	457.2	10	4.4	8.4-9.7	0.53	10, 20 and 30	0.52-1.44
ENODISE	305	2	1	11-22	0.048	30	1

Specifically, this paper aims at predicting boundary-layer–propeller interaction noise by considering two effects: i) the interaction of the propeller with the mean flow inhomogeneity, and ii) the reflections by the underlying flat plate. The analysis is supported by experimental data.

2. Methods

2.1 Experimental setup

The experiments were carried out at the Universities of Bristol and Twente in their respective open-jet wind tunnel. In both cases the anechoic chamber has a cutoff frequency of 160 Hz. The setups share the same propeller design. The boundary layer develops over a flat plate and is triggered by a tripping device. Two arrays of microphones were placed outside the freestream respectively above the plate and sideline as illustrated in Fig. 1. The Cartesian system of coordinates (x, y, z) is used, with x indicating the streamwise direction (pointing downstream), y, the lateral direction in the plane of the flat plate, and z the direction perpendicular to the plate pointing to the sky. The propeller rotation is negative in the (y, z)-plane. In this paper, the polar angle Ψ is defined such as $\Psi = 0°$ at the rear and $180°$ at the front.

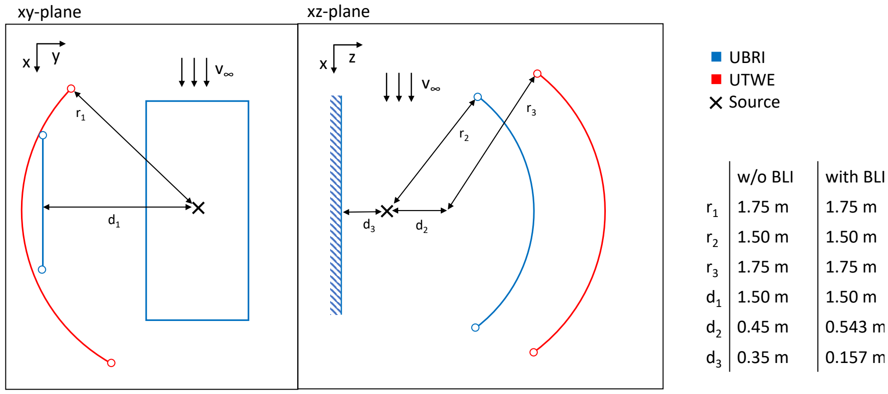

Figure 1: Microphone arrangement (not to scale).

The position $\Psi = 90°$ denotes positions in the propeller plane.

The 2-bladed propeller (diameter D =304.8 mm) was designed by Mejzlik from a modified NACA4412 profile. It was operated at an advance ratio $J \approx 1$ with $J = U_\infty/nD$, where U_∞ is the freestream velocity at the edge of the boundary layer and n the rotation speed. The propeller (driven electrically) was perfectly aligned with the mean flow. The gap between the tip and the flat plate was fixed to 5 mm.

2.1.1 Specifics of the setup of Bristol University

The setup of Bristol is described in detail by Zaman et al. [7, 8]. The wind-tunnel exit has a 775 mm×500 mm cross-section. The turbulence intensity is 0.12% in the jet core. The flat plate, on which the boundary layer develops, is 2 m wide and 1.69 m long in the streamwise direction. The edges are covered with porous material to minimise blunt trailing-edge noise and also reduce acoustic diffraction. The tripping device is a porous strip of 25 mm×10 mm cross-section placed 1000 mm upstream of the propeller. The signals were recorded during 32 s at a sampling rate of 2^{16} Hz. The boundary layer was characterised by hot wire anemometry. The main information on the boundary layer (see shape in Fig. 2) is summarised in Table 2. The microphone arrangement comprised a semi-circular array of 25 mics placed above the plate in the (x, z)-plane and a semi-circular array of 23 mics placed on the right side of the propeller in the (x, y)-plane (see Fig. 1). The measured acoustic spectra exhibit clear peaks at least up to the 2×BPF as shown exemplarily in Fig. 3.

2.1.2 Specifics of the setup of Twente University

The setup of the experiments performed at Twente is described in detail by Castelucci et al. [9]. The wind tunnel has a 900 mm×700 mm cross-section. The turbulent intensity is below 0.1%. Two types of boundary layer tripping devices were used with 60° zigzag trips. They were placed at 3600 mm upstream of the propeller plane. The microphone arrangement comprehended two arrays: a semi-circular array of

Table 2: Differences between the boundary layers.

Owner	tripping	U_∞	δ_{99}	immersion depth
UBRI (blue)	10 mm porous trip	30 m/s	0.1015 m	≈32%
UTWENTE (orange)	8 mm zigzag trip	30 m/s	0.103 m	≈32%
UTWENTE (green)	12 mm zigzag trip	30 m/s	0.14 m	≈44%

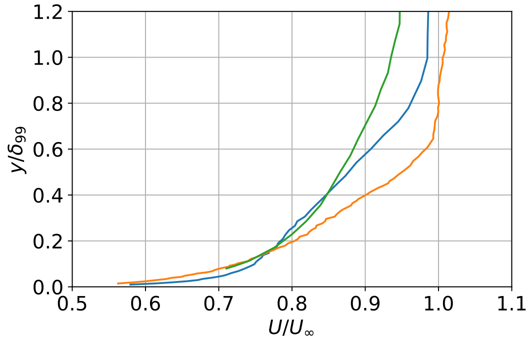

Figure 2: Boundary layers; (blue) Bristol, (orange) trip 1 and (green) trip 2 from Twente.

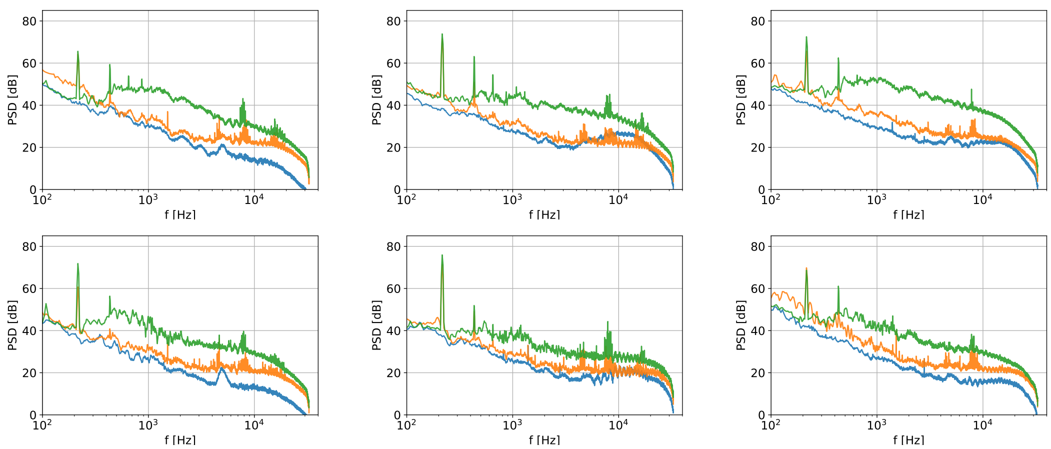

Figure 3: Microphone spectra measured at Bristol in the (top) (x, y) and (bottom) (x, z)-planes; (left) forward arc, (middle) sideline, (right) rear arc; (orange) propeller isolated, (green) propeller immersed in the boundary layer, (blue) background noise of the BLI configuration.

17 mics placed above the plate and a line array of 10 mics placed on the right side of the propeller parallel to the propeller axis. The measured acoustic spectra exhibit peaks up to the 2xBPF as shown in Fig. 4.

2.2 Prediction method

2.2.1 Approach

The far-field pressure fluctuations p' shall be compared to the microphone measurements. It is assumed that the pressure can be decomposed into a periodic $\tilde{p}$ and a non-periodic component p'':

$$p'(t) = \tilde{p}(t) + p''(t) \tag{1}$$

This work is focused on the periodic part. It is assumed that the problem can be linearised and the noise generation be modelled as the sum of two source mechanisms. The first mechanism represents the steady components (lift, drag, thickness) produced by the propeller as it were alone and the second mechanism is due to the interaction of the blades with the mean inflow distortion as sketched in Fig. 5:

$$\tilde{p}(t) = \tilde{p}_p(t) + \tilde{p}_{bl-p}(t) \tag{2}$$

Finally the method of image is used to account for the flate plate reflections.

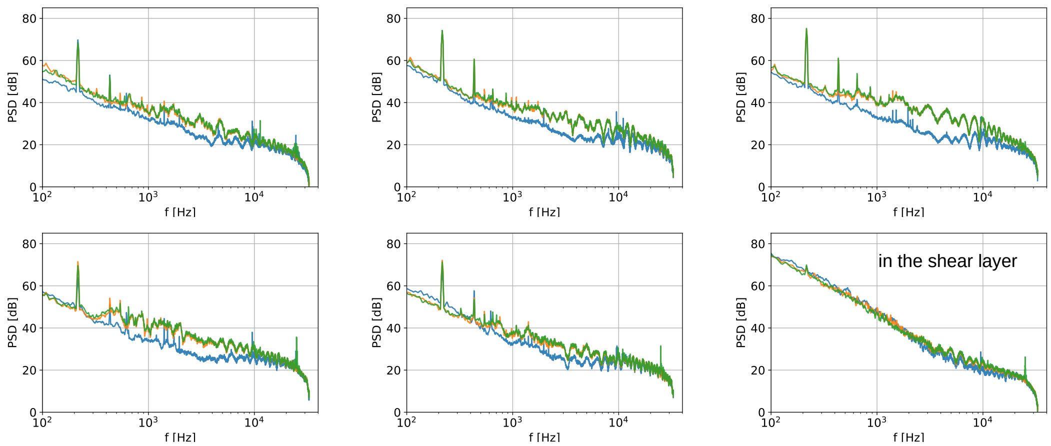

Figure 4: Microphone spectra measured at Twente in the (top) (x, y) and (bottom) (x, z)-planes; (left) forward arc, (middle) sideline, (right) rear arc; (blue) propeller outside the boundary layer, (orange) propeller in the boundary layer (trip 1), (green) propeller in the boundary layer (trip 2).

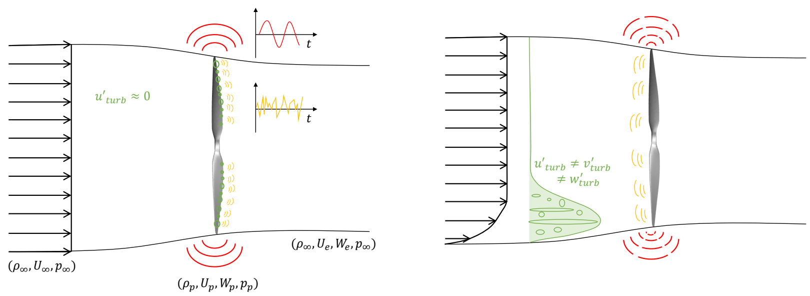

Figure 5: (Left) Noise generation by the isolated propeller, (right) noise generation by the propeller interacting with the boundary layer flow.

2.2.2 Blade element momentum theory

The blade element momentum theory was applied to obtain the lift and drag coefficients as well as the mean flow components needed for the analytical models. A decent agreement in terms of global performance (see Fig. 6) can be achieved if the viscosity effects on the blade (in particular the laminar–turbulent transition) is considered. For that reason, the program XFOIL [10] was used to calculate the coefficients of lift and drag against angle of attack for the 2D profiles extracted at several radial positions. The Ncrit criterium was set to the value 9, which corresponds to a moderate inflow turbulence. The swirl of the propeller was considered in the momentum theory. Finally, a tip vortex correction was applied.

2.2.3 Tonal noise generation and reflections by the plate

Using the aerodynamic output of BEMT, the prediction of rotor-alone tonal noise is performed as if the propeller were embedded in a uniform flow:

$$\tilde{p}_p(t) \approx \tilde{p}_L(t) + \tilde{p}_D(t) + \tilde{p}_T(t). \tag{3}$$

The three terms in Eq.3 describe the lift, drag and thickness noise components, respectively. The farfield analytical solutions implemented in the in-house program PropNoise are used (see Moreau and Guérin ([11]). They have been validated for high-speed propellers [12, 13]. The interaction tones are predicted using the acoustic response of a flat (rotating) plate to a sinusoidal gust.

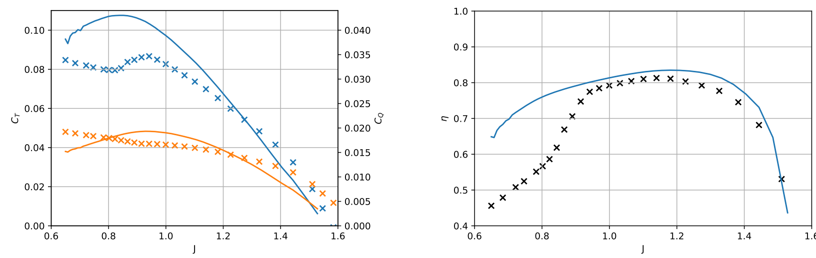

Figure 6: (blue) Thrust, (orange) torque and efficiency η of the propeller; (x) Bristol data, (–) BEMT.

Acoustic reflections by the plate are modelled using the method of image, that is, the plate is assumed infinite in all directions. The image of the propeller is a second propeller rotating in the opposite direction. The formulation by Guérin and Tormen [13] to calculate the acoustic interference between distributed propellers is applied. Note, however, that the refraction by the wind-tunnel shear layer is ignored.

3. Results

3.1 Isolated propeller (without BL interaction)

For a propeller alone, the steady-lift component is dominant as shown in Fig. 7 at BPF and 2×BPF. The agreement to the Bristol experiments (performed without flat plate) is satisfactory. The measurement at Twente were performed while the plate was still mounted. In that case, it appears that considering the acoustic reflections by the plate slightly improves the results for the mics above the plate (see Fig. 8).

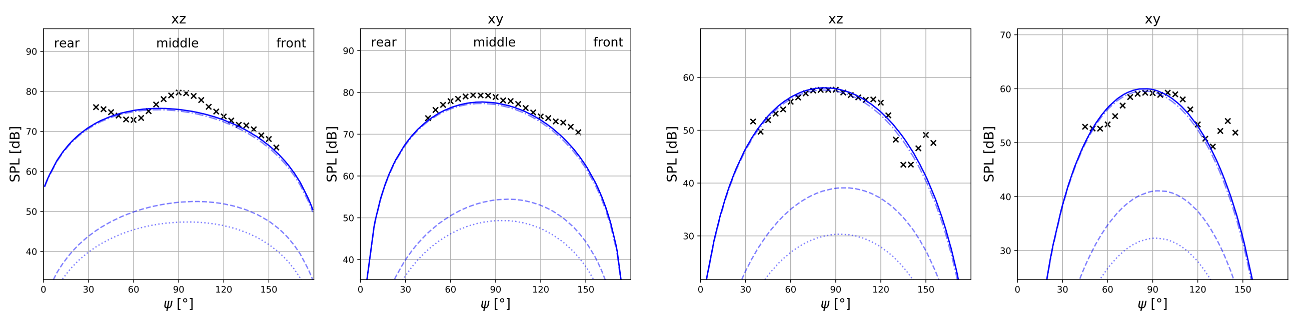

Figure 7: Comparison for the propeller alone without plate: (x) Bristol experimental data, (solid line) steady lift, (dashed line) thickness, (dotted line) steady drag noise; (left) BPF, (right) 2×BPF.

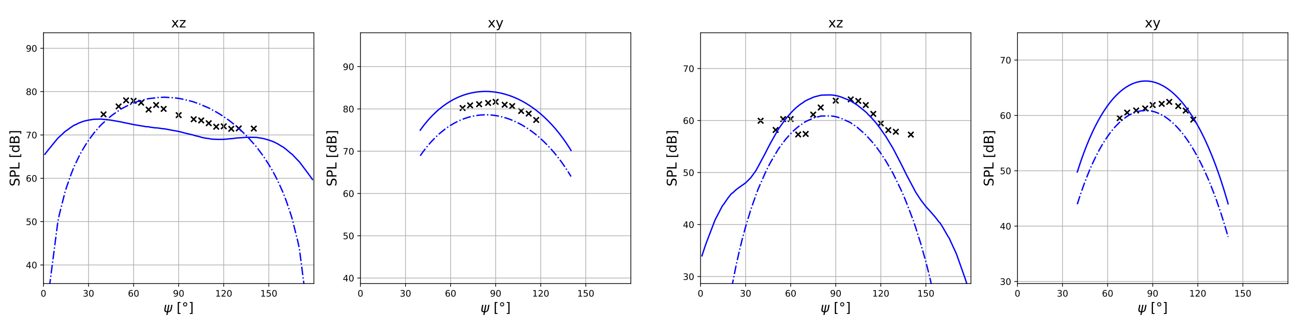

Figure 8: Comparison for the propeller without BLI but with installed plate: (x) Twente experimental data, (dashed line) without, (solid line) with reflections by the plates; (left) BPF, (right) 2×BPF.

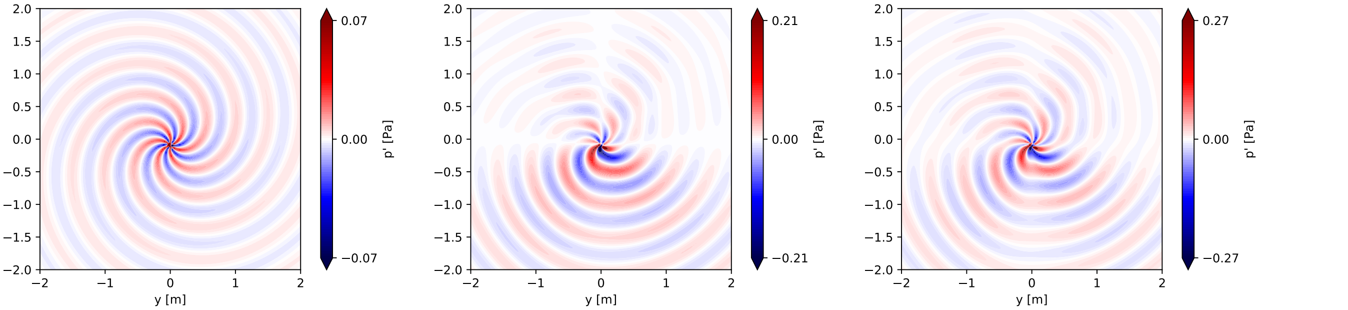

Figure 9: Noise generation by (left) the isolated propeller and (middle) the propeller interacting with the boundary layer flow, (right) sum of the two components; 3×BPF, without propeller image.

3.2 Propeller with BL interaction

An example of the predicted pressure field is showed in Fig. 9 at 3×BPF, for which BLI is dominant. The sum of the steady-lift component and the BL interaction can give rise to further interferences.

A comparison of the experimental results with BLI in Fig. 10 and 11 with those without BLI in Fig. 7 and 8 indicates that the acoustic levels with BLI only little increase at BPF whereas they are significantly higher by up to 10 dB at 2×BPF. The predictions overestimate the absolute levels, however the results are interesting for two reasons. Firstly, they show that the relative contribution of BLI noise increases rapidly with the BPF index. Secondly, the directivity patterns contain radiation nodes due to interference, which are also clearly visible in the experiments. The fact that BLI is overestimated may be due to the fact that the blade profiles are thick and therefore less noisy that what the flat plate theory predicts.

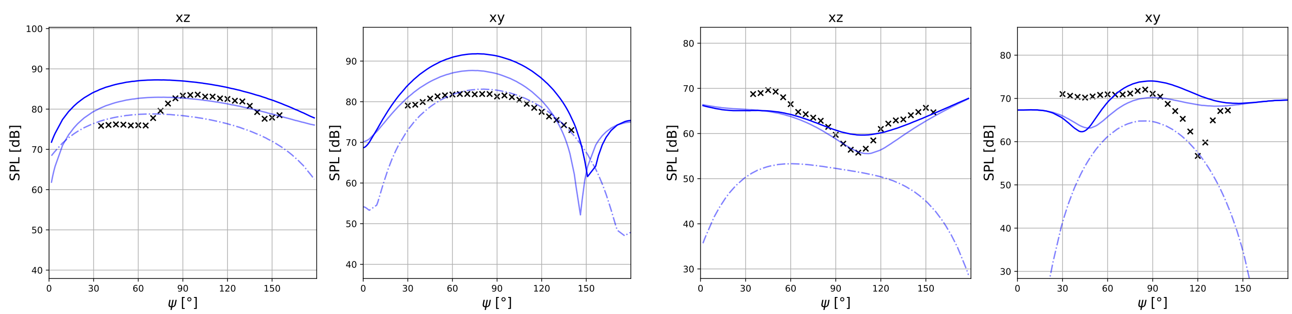

Figure 10: Results with BL interaction; (x) Bristol experimental data, (dashed line) steady-lift contribution, (thin line) BL interaction, (thick line) sum of the two contributions; (left) BPF, (right) 2×BPF.

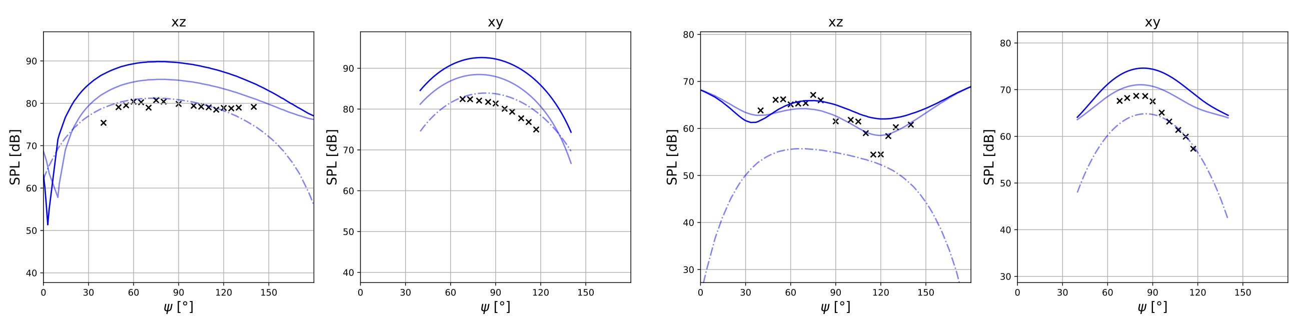

Figure 11: Results with BL interaction; (x) Twente experimental data (same legend as in Fig. 10).

4. Conclusion

This study has shown that sharp acoustic tones are present in the ENODISE A1 data contrary to what was observed in other BLI experiments with more rotor blades. The acoustic analogy has been coupled to BEMT to predict the propeller alone tones and a good agreement has been found. Regarding the BL interaction with the rotor, it has been assumed that it can be modelled as a gust–airfoil interaction source. Predictions and experiments show the same trends, in particular they indicate that the relative contribution of BLI noise increases with the BPF harmonic index. Considering the reflections by the flat plate has helped improve the prediction, primarily for the mics above the plate. Radiation nodes are present in the directivity patterns, which is a clue of acoustic interference. The overestimation of BLI noise may be due to the fact that the blades are thick, whereas the theory assumes thin flat profiles.

5. Acknowledgements

The work is supported by the European Union's Horizon 2020 research and innovation program under the ENODISE (Enabling optimized disruptive airframe-propulsion integration concepts) project grant agreement No. 860103.

REFERENCES

1. ENODISE (Enabling optimized disruptive airframe-propulsion integration concepts), https://www.vki.ac.be/index.php/about-enodise (accessed 31.03.2023).

2. D.B. Hanson, Spectrum of rotor noise caused by atmospheric turbulence, J. Acoust. Soc. Am. 56(1) (1975), pp. 110–126.

3. W.N. Alexander and W.J. Devenport, S.A.L. Glegg, Noise from a rotor ingesting a thick boundary layer and relation to measurements of ingested turbulence, J. Sound Vib., 409, 227-240, 2017.

4. H.H. Murray IV, W.J. Devenport, W.N. Alexander, S.A.L. Glegg, D. Wisda, Aeroacoustics of a rotor ingesting a planar boundary layer at high thrust, J. Fluid Mech. (2018), vol. 850, pp. 212–245.

5. L.Klähn, L. Caldas, U. Tapken, Measurements of fan inflow distortion noise generation in a low speed fan – part II: acoustic analyses, 28th AIAA/CEAS Aeroacoustics 2022 Conference, Southampton, UK, June 14-17, 2022.

6. L. Klähn, L. Caldas, R. Meyer, A. Moreau and U. Tapken, Experimental investigation of inflow-distortion-induced tonal noise in a sub-sonic fan test rig. 29th International Congress on Sound and Vibration, 2023, Prague (CZ).

7. I. Zaman, M. Falsi, B. Zang, M. Azarpeyvand, R. Camussi, Experimental Investigation of the Haystacking Phenomenon for Propeller Boundary Layer Ingestion, 2023 AIAA Aviation Forum, San Diego (CA), USA, June 2023.

8. I. Zaman, M. Falsi, B. Zang, M. Azarpeyvand, R. Camussi, Effect of Tip Gap on Nearfield and Farfield Acoustics of Propeller Boundary Layer Ingestion, 2023 AIAA Aviation Forum, San Diego (CA), USA, June 2023.

9. L.A. Castelucci, C.H. Venner, L.D. de Santana, Experimental analysis of the noise of small propellers subjected to non-uniform inflow, AIAA SCITECH 2023 Forum, National Harbor (MD), USA, January 2023.

10. http://web.mit.edu/drela/Public/web/xfoil/ (accessed 31.03.2023).

11. A. Moreau, S. Guérin, Similarities of the in-duct and free-field formulations in rotor noise problems, 17th AIAA/CEAS Aeroacoustics Conference (32nd AIAA Aeroacoustics Conference), Portland, USA, 05-08 June 2011.

12. S. Guérin, A. Moreau, C. Menzel, C. Weckmüller, Open-rotor noise prediction with a RANS-informed analytical method, 18th AIAA/CEAS Aeroacoustics Conference, Colorado Springs (CO), USA, June 2012.

13. S. Guérin, D. Tormen, Noise radiation by eight wingspan-distributed propellers, Deutscher Luft- und Raumfahrtkongress, Dresden, Germany, September 2022.